Optical Devices Constructed from Ferrocene-Modified Microgels for H_2O_2 Sensing

Qiang Matthew Zhang,[a] Darren Berg,[b] Jiaqi Duan,[a] Samuel M. Mugo,[b] and Michael J. Serpe*[a]*

a. Department of Chemistry, University of Alberta, Edmonton, AB, T6G 2G2 Canada. E-mail: michael.serpe@ualberta.ca; Tel: +1 780 492 5778; Fax: +1 780 492 8231.

b. Physical Sciences Department, MacEwan University, Edmonton, AB, T5J 4S2 Canada. E-mail: mugos@macewan.ca; Tel: +1 780 887 7026

Keywords: Microgels, Optical devices, H_2O_2 sensing, Responsive polymer, Glucose Sensing

ABSTRACT: Ferrocene-modified poly (N-isopropylacrylamide) - based microgels were synthesized, characterized and used to construct optical devices (etalons). The response of the microgels and etalons to H_2O_2 was investigated, and we show that both the microgel diameter, and the optical properties of the etalons, depended on the solution concentration of H_2O_2 from 0.6 mM to 35 mM. This behavior is a direct result of the oxidation of ferrocene, which influences the microgel diameter. This was also demonstrated by electrochemical-mediated oxidation/reduction of ferrocene using cyclic voltammetry. We go on to show that these materials could be used to monitor H_2O_2 that is generated from enzymatic reactions. Specifically, we show that the H_2O_2 generated from the oxidation of glucose catalyzed by glucose oxidase could be quantified. Finally, the devices can be reused multiple times via a regeneration process. This investigation illustrates the versatility of the etalon system to detect species of broad relevance, and how they could potentially be used to quantify products of biological reactions.

1. INTRODUCTION

Hydrogen peroxide (H_2O_2) plays a vital role in the regulation of many physiological processes, and is the by-product of many metabolic processes in living organisms. Generally, changes in H_2O_2 homeostasis can affect cell proliferation, death and signal transduction.[1] However, excessive amounts of H_2O_2 in the human body has been linked to irreversible oxidative damage, causing aging,[2] neurodegeneration,[3] DNA damage, [4] and cancer.[5] Due to the significant role of H_2O_2 in biological processes, determination of the concentration of H_2O_2 in samples is of critical importance. To date, various analytical techniques have been developed that are capable of H_2O_2 quantitation, such as chemiluminescence,[6] spectrophotometry,[7] fluorescence,[8] and electrochemical methods.[9] In one case, platinum based amperometric sensors have been developed to detect H_2O_2, which exhibited high sensitivity and low limit of detection

due to the high catalytic activity of the platinum nanoparticles.[10] Through combination with enzymes, the application of amperometric biosensors was extended to sense various biomolecules via determining H_2O_2 levels generated from enzymatic reactions.[11-13] While each of these approaches have their own benefits, some are time consuming to implement, require expensive reagents/instrumentation, a laboratory setting, and trained personnel.[14] In particular, electrochemical methods while sensitive suffer from electrode poisoning and chemical interferences.

Over the past few decades, photonic materials have emerged as useful sensing motifs that can provide alternatives to the traditional sensors mentioned above. This is in part due to their low cost, ease of signal readout (a visual color change), simple operation, and straightforward modification to allow the detection of multiple analytes.[15] The Asher group demonstrated in many publications that two-dimensional photonic crystals could be fabricated by entrapping colloidal particles packed in an ordered array in a responsive polymer-based hydrogel matrix.[16,17] They went on to show that the materials could be used for sensing and biosensing.[18] Relatedly, many three-dimensional photonic crystals have also been developed and used to detect various analytes, such as pH,[19] alcohols,[20] cholesterol,[21] bacteria,[22] and tetracycline.[23] Our group published the first report of a specific microgel-based optical device construct (i.e., an etalon) in 2010 (Scheme 1a).[24,25] We have investigated their optical properties in many subsequent publications, and showed that their optical properties change in response to the environment and the presence of certain analytes, e.g., solution temperature and pH,[26] triglycerides,[27] Tabun,[28] Cu^{2+},[29] CO_2,[30] protein,[31] and DNA[32]. In short, etalons are constructed by "painting" a concentrated microgel solution on an Au-coated glass substrate, followed by copious rinsing with deionized water to remove microgels not directly attached to the Au.[33] Finally, the microgel

layer is dried, and an additional layer of Au deposited on the microgel layer. The optical properties of the devices can be predicted by eqn (1):

$$m \lambda = 2 n d \cos \theta \qquad (1)$$

where (n) is the refractive index of the dielectric layer, (d) is the Au–Au distance, (θ) is the angle of incident light relative to the normal, and (m) is the order of the reflected peak (can be any integer). Therefore, the position of the peaks in reflectance spectra (and hence the device color) depends on the distance between two Au layers and the refractive index of microgels (at a single observation angle).[33] Furthermore, the device color (and optical properties) depends primarily on the distance between the two Au layers.[25] In this paper, we demonstrate that etalons could be fabricated that change optical properties in response to H_2O_2, and were subsequently used to quantify H_2O_2 concentration in solutions (Scheme 1a).

(a)

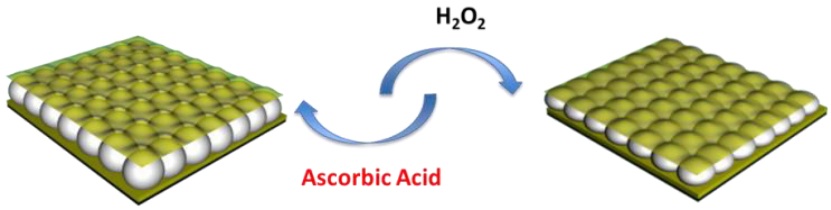

(b)

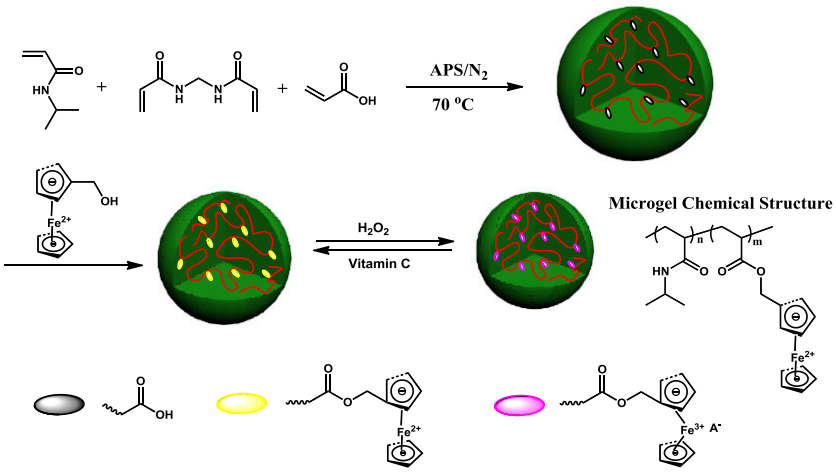

Scheme 1. (a) Etalon structure and responsivity. In presence of H2O2, the distance between the two gold layers decreases, which leads to a blue-shift in the peaks of the reflectance spectra. The peaks in the reflectance spectra return to their original position upon exposure to ascorbic acid. (b) Microgel synthesis scheme, and resulting microgel chemical composition.

2. EXPERIMENTAL SECTION

2.1 Measurements

Transmission electron microscope (TEM) images were obtained on an ultrahigh-resolution transmission electron microscope (JEOL JEM-2010FEF) using an accelerating voltage of 200 kV. Reflectance measurements were conducted using a USB2000+ spectrophotometer, a HL-2000-FHSA tungsten light source, and a R400-7-VISNIR optical fiber reflectance probe, all from Ocean Optics (Dunedin, FL). The spectra were recorded using Ocean Optics Spectra Suite Spectroscopy Software over a wavelength range of 400–1000 nm. Dynamic light scattering (DLS) measurements were carried out by using a DLS/SLS-5000 compact goniometer (ALV, Langen) coupled with an ALV photon correlator. Electrochemical experiments were carried out using an auto-lab electrochemical workstation at room temperature with a three-electrode setup; the etalons top and bottom Au layers were used as the working, and auxiliary electrodes, respectively. A homemade Ag/AgCl electrode was used as the reference electrode. The experiments were conducted using a scan rate of 10 mV s^{-1} in a pH = 7 buffer solution (0.1 M NaH_2PO_4/Na_2HPO_4 and 0.1 M KCl).

2.2 Synthesis of carboxylic acid containing microgels (MG-AAc).

A 3-necked round bottom flask was fitted with a reflux condenser, nitrogen inlet, and temperature probe, and charged with a solution of N-isopropylacrylamide (11.9 mmol), acrylic acid (0.65 mmol), and N,N'-methylenebisacrylamide (0.65 mmol) in 99 mL deionized (DI) water, previously filtered through a 0.2 μm filter. The solution was purged with N_2 gas while being

heated to 70 °C. The reaction was then initiated by addition of a solution of ammonium persulfate (0.2 mmol) in 1 mL of deionized water. The reaction proceeded at 70 °C for 4 h under a blanket of nitrogen. The resulting suspension was allowed to cool while stirring, and then filtered through Whatman #1 filter paper to remove any large aggregates. The microgel solution was then distributed into centrifuge tubes and purified via centrifugation at ~8300 rcf to form a pellet, followed by removal of the supernatant and resuspension with deionized water; this process was repeated 6 times. The cleaned microgels were recombined and stored in a brown glass jar.

2.3 Synthesis of ferrocene containing microgels (MG-Fe).

To a solution of MG-AAc (AAc composition is 0.1 mmol) in anhydrous DMF was added ferrocenylmethanol monomer (0.3 mmol). After complete dissolution, 1-ethyl-3-(3-dimethyllaminopropyl) carbodiimide hydrochloride (EDC-HCl, 0.2 mmol) and a catalytic amount of 4-(dimethylamino) pyridine (DMAP) were added into the stirred solution. The reaction mixture was allowed to react at room temperature for 2 days. The microgel solution was then distributed into centrifuge tubes and purified via centrifugation at ~8300 rcf to form a pellet, followed by removal of the supernatant and resuspension in fresh DMF 6 times, followed by centrifugation and resuspension in DI water 3 times. The cleaned microgels were recombined and stored in a single brown glass jar. The amount of unreacted AAc was determined by titration using NaOH and methyl red as indicator.

2.4 Etalon preparation.

Etalons were fabricated using techniques previously reported elsewhere.[31] In short, 25 x 25 mm ethanol rinsed and N_2 gas dried microscope coverslips (Fisher's Finest, Ottawa, ON) were coated with 2 nm Cr followed by 15 nm of Au via thermal evaporation at a rate of 1 Å s^{-1}, and

0.1 Å s^{-1}, respectively (Torr International Inc., thermal evaporation system, Model THEUPG, New Windsor, NY). The Cr/Au substrates were annealed in a Thermolyne muffle furnace at 250 °C for 3 h and cooled to room temperature prior to microgel film deposition. Then, a 40 μL aliquot of concentrated microgels was spread onto an annealed 25 mm x 25 mm Au-coated glass coverslip. The film was allowed to dry on a 30 °C hotplate for 30 minutes before the excess microgels not bound directly to the Au layer were rinsed away with DI water. The samples were then soaked overnight at 30 °C in a DI water bath. The samples were then rinsed with DI water, dried with N_2 gas, and another Au layer (2 nm Cr for adhesion, followed by 15 nm Au) was added. The completed device was soaked overnight in DI water at 30 °C before use.

3. RESULTS AND DISCUSSION

First, ferrocene-modified microgels were synthesized, and used to construct etalons. Briefly, MG-AAc microgels were synthesized via free radical precipitation polymerization of N-isopropylacrylamide, acrylic acid, N,N'-methylene bis(acrylamide) (crosslinker), as shown in Scheme 1b. Then, ferrocene was covalently attached to the microgels via reaction of ferrocenylmethanol with the carboxylic acids on/in the microgels. Following the esterification reaction, the pH of the microgel solution changed from 4.2 to 6.8, which is indicative of the acrylic acid being converted to the ester. The amount of unreacted carboxylic acid on the microgels was determined by titration with NaOH (0.01 M) using methyl red as an indicator. From these data, we determined that the amount of unreacted carboxylic acid was below 0.2%. TEM images of the microgels are shown in Figure 1. As can be seen, the microgels are spherical, with average dry diameters of 400 nm (± 10 nm) for MG-AAc and 340 nm (± 8 nm) for MG-Fe^{2+}. The diameter of the solvated microgels was characterized by DLS (Figure S1). DLS revealed hydrodynamic diameters of 730 nm (± 12 nm) for MG-AAc and 550 nm (± 8 nm) for

MG-Fe^{2+} at 30 ^{o}C. These values are averages of three repeat analyses of the microgel solution. The decrease of the diameter after the esterification reaction was attributed to the increased microgel hydrophobicity by replacing the carboxylic acid with the relatively hydrophobic ferrocene.

The responsivity of MG-Fe to H_2O_2 was subsequently investigated. In the presence of H_2O_2, the microgel diameter decreased to 120 nm in dry state (Figure 1c) and 290 nm in swollen state (Figure S1). We attribute the decrease in diameter to the interaction of the polar amide groups of the microgels with the 1+ charge on ferrocene. That is, when MG-Fe was exposed to H_2O_2, the Fe^{2+} of ferrocene could be oxidized to Fe^{3+} causing it to transition to a +1 charge state.[34] This phenomenon was also observed for hydrogels composed of anionic poly (ferrocenylsilane).[35]

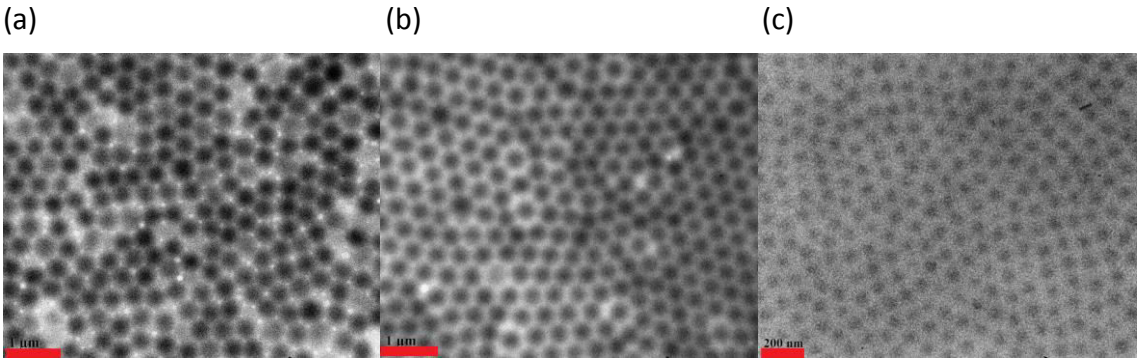

Figure 1 TEM images of (a) MG-AAc (scale bar is 1 μm), (b) MG-Fe^{2+} (scale bar is 1 μm), (c) MG-Fe^{3+} (scale bar is 200 nm).

With the response of the microgels to H_2O_2 verified, they were subsequently used to construct microgel-based etalons and their response to H_2O_2 exposure determined. The reflectance spectrum of a resultant device at 30 ^{o}C can be seen in Figure 2. As can be seen, a characteristic multipeak reflectance spectrum was observed, with peaks at 561 nm, 655 nm, and 786 nm at 30 ^{o}C. From the relative positions of the reflectance peaks, and using eqn (1), the order (m) of each peak can be calculated. The peak at 786 nm is m = 5 (noted as λ_5), λ_6 is 655

nm, while λ_7 is 561 nm. When conducting these experiments, it is important to compare the same order reflectance peaks before and after introduction of H_2O_2. As can be seen in Figure 2a, a 95 nm total blue shift of λ_5 could be observed after exposure to 11.8 mM H_2O_2. We note that a detectable change is observed within 5 min, although it takes ~20 min for the signal to stabilize (Figure S2). Furthermore, as the H_2O_2 concentration increased from 0.6 mM to 35 mM, λ_5 blue-shifted from 10 nm to 155 nm, with the signal saturating at 35 mM (Figure 2b). The limit of detection of the etalon was calculated to be ~ 40 μM H_2O_2. As a control, etalons were constructed from pNIPAm-based microgels that did not contain ferrocene, and exposed to H_2O_2; these devices had relatively little response to H_2O_2 (Figure S3). This demonstrates that the blue-shift of the MG-Fe etalons was due to the oxidation of ferrocene by H_2O_2. In order to explore the function of the etalons in more complex environments, their response to H_2O_2 was also investigated in presence of 15 ppm ascorbic acid (physiological levels are ~0.08 mM). We found that in this case the etalon's response to H_2O_2 was virtually unaffected by the presence of ascorbic acid (Figure S4 and S5). Furthermore, the etalons exhibited similar response behaviour to H_2O_2 in milk (1:100 dilution), as shown in Figure S6.

(a)

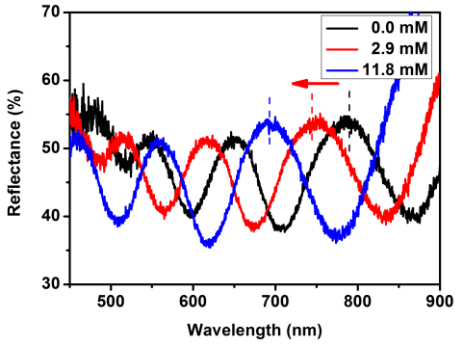

(b)

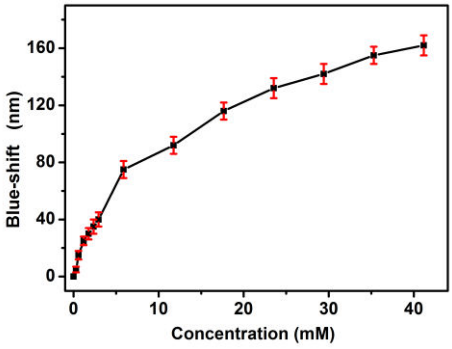

(c)

(d)

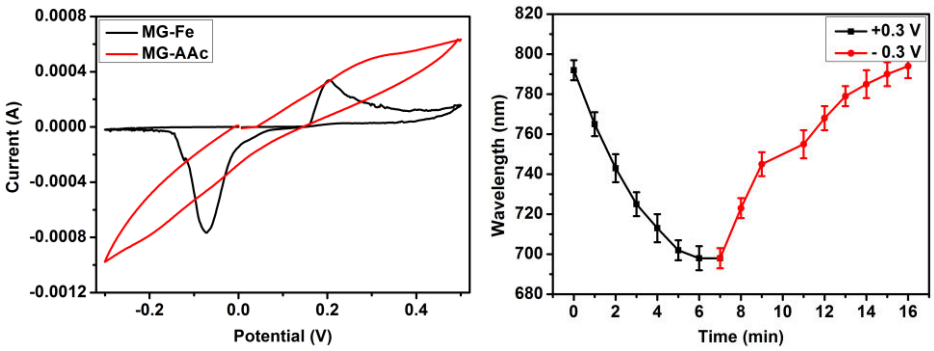

Figure 2 (a) Reflectance spectra of etalon upon exposure to the indicated concentrations of H_2O_2, the direction of the peak shift is indicated with the red arrow; (b) λ_5-Peak shifts as function of H_2O_2 concentration; (c) Cyclic voltammetry of the MG-Fe and MG-AAc etalons using homemade Ag/AgCl as reference electrode; (d) λ_5 as function of time at the indicated potentials. The etalon was immersed in pH 7 buffer solution (NaH_2PO_4/Na_2HPO_4).

The electrochemical properties of the redox active MG-Fe were also studied using cyclic voltammetry (CV) in a pH = 7 buffer solution (0.1 M NaH_2PO_4/Na_2HPO_4 and 0.1 M KCl). The two Au layers were used as working and auxiliary electrodes. Figure 2c shows the CV for an etalon composed of MG-Fe. As can be seen, anodic and cathodic peaks were observed at 0.20 V and -0.07 V, respectively, which is near what is expected for ferrocene (0.17 V/0.047 V). The large redox peak separation could be the result of sluggish electron transfer kinetics as a result of the presence of the microgel dielectric layer. For comparison, the CV of a MG-AAc etalon was also obtained, which showed no redox peaks. The diagonal voltammetric response of MG-AAc etalon was due to resistance as a result of non-conductive dielectric microgel layer near the conductive thin porous gold film. This phenomenon was eliminated by presence of redox species-ferrocene in MG-Fe. Therefore, it could be concluded that the redox peaks for the MG-Fe etalon were related to the oxidation and reduction of the ferrocene in the microgels. We then investigated how the optical properties of the etalons depended on the oxidation state of the ferrocene. To do this, the optical properties of the etalons were monitored using reflectance spectroscopy. As can be seen in Figure 2d, when the microgels were oxidized at + 0.3 V, λ_5 blue shifted 85 nm within 6 mins. Furthermore, when the microgels were reduced at – 0.3 V, λ_5

returned to its original position. Again, this change is a result of the microgels size modulating the distance between the etalons Au layers, which ultimately depends on the oxidation state of ferrocene.

Next, we determined the ability of MG-Fe etalons to quantify H_2O_2 concentration in solution. As a reactive oxygen species, H_2O_2 is generated from nearly all biological oxidative cycle reactions and has the ability to diffuse in and out of cells and tissues.[36] For example, choline oxidase catalyzes the oxidation of choline in the presence of oxygen, which produces betaine aldehyde and H_2O_2.[37] H_2O_2 is also a metabolic product of lactate oxidation reaction catalyzed by lactate oxidase.[38] Therefore, the detection of H_2O_2 can be used to indirectly monitor various biological enzymatic reactions. In this submission, the enzymatic reaction between glucose oxidase and glucose, which generates H_2O_2, was chosen as model reaction. Specifically, glucose can be oxidized by glucose oxidase in the presence of O_2 to generate H_2O_2 and gluconic acid (Figure 3a). H_2O_2 has been shown to be stable in human cells for 6 h, and therefore its detection in solution is feasible.[39,40] To conduct this study, MG-Fe containing etalons were exposed to various concentrations of glucose in presence of glucose oxidase (0.1 mg mL^{-1}), and the reflectance spectra collected as a function of time. As can be seen in Figure 3b, λ_5 blue-shifts as the reaction time increases, and stabilizes at ~2 h. Furthermore, the magnitude of the blue shifts increased from 67 nm to 163 nm, as the glucose concentration increased from 2.2 mM to 7.8 mM (Figure 3c). This was a direct result of the H_2O_2 generated from the glucose oxidation oxidizing the ferrocene, which causes the microgels to collapse; the extent of the collapse is proportional to glucose concentration, which is directly related to H_2O_2 concentration. The etalon exhibited similar response kinetics toward glucose in presence of physiological levels of ascorbic acid, indicating that the etalon could be used to test glucose in real samples (Figure S7). We

point out that the blood glucose level recommended by National Institute for Clinical Excellence is in the range of 3.9-5.5 mM. Therefore, the device can respond in a physiologically relevant range. Finally, since the oxidation/reduction of Fe^{2+}/Fe^{3+} is reversible, the microgel diameter (and etalon optical properties) can be returned to their initial state by the reduction of ferrocene, which can be done by exposure to reducing agents or appropriate reduction potentials. In this study we showed that the etalons optical properties were reversible over many cycles upon exposure to ascorbic acid (reduction) at concentration of 1000 ppm and reoxidation (Figure S8).[41] The stability of etalon was also evaluated by determining its glucose response after freezer storage. We found no obvious performance loss after 4 weeks storage (Figure S9).

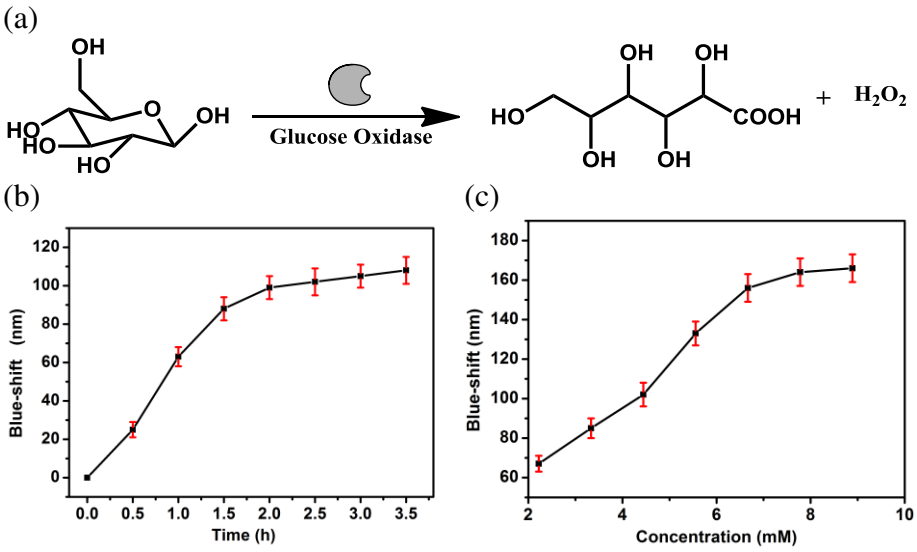

Figure 3 (a) Glucose oxidation reaction catalyzed by glucose oxidase; (b) Peak shifts as function of time upon exposure to 4.4 mM glucose; (c) Peak shifts as function of glucose concentration. The experiment was conducted in pH 7 buffer solution (NaH_2PO_4/Na_2HPO_4).

4. CONCLUSIONS

In summary, ferrocene-containing microgels were synthesized, and etalons fabricated by sandwiching them between two thin Au layers. The resultant microgels, and etalons, were shown to H_2O_2 exposure by shrinking in a manner that depended on H_2O_2 concentration. Furthermore,

we showed that the response to H_2O_2 concentration was linear in the range of 0.6-35 mM. Finally, we showed that H_2O_2 generated from biological enzymatic reactions could be detected using the H_2O_2-responsive etalons. Due to their low cost of ~$0.1 CAD per square inch and ease of use, these devices could find various real world applications.

ACKNOWLEDGEMENTS

MJS acknowledges funding from the University of Alberta (the Department of Chemistry and the Faculty of Science), the Natural Sciences and Engineering Research Council of Canada (NSERC), the Canada Foundation for Innovation (CFI), the Alberta Advanced Education & Technology Small Equipment Grants Program (AET/SEGP), Grand Challenges Canada and IC-IMPACTS. Q. Zhang acknowledges financial support through an Alberta Innovates Technology Futures (AITF) Postdoctoral Fellowship. SMM acknowledges MacEwan Research for Funding. MJS acknowledges Mark McDermott for the use of the thermal evaporator.

ASSOCIATED CONTENT

Supporting Information

The Supporting Information is available free of charge on the ACS Publications website. Characterization methods, microgel synthesis scheme, dynamic light scattering measurements of microgel diameter, and optical microscope images.

AUTHOR INFORMATION

Corresponding Author

*M. J. Serpe E-mail: michael.serpe@ualberta.ca

*S. M. Mugo E-mail: mugos@macewan.ca

REFERENCES:

1. Lindahl, T. Instability and Decay of the Primary Structure of DNA. *Nature* **1993,** *362* (6422), 709-715.

2. Dröge, W.; Schipper, H. M. Oxidative Stress and Aberrant Signaling in Aging and Cognitive Decline. *Aging Cell* **2007,** *6* (3), 361-370.

3. DiMauro, S.; Schon, E. A. Mitochondrial Disorders in the Nervous System. *Annu. Rev. Neurosci.* **2008,** *31*, 91-123.

4. Troll, W.; Wiesner, R. The Role of Oxygen Radicals as a Possible Mechanism of Tumor Promotion. *Annu. Rev. Pharmacool. Toxicol.* **1985,** *25* (1), 509-528.

5. Finkel, T.; Serrano, M.; Blasco, M. A. The Common Biology of Cancer and Ageing. *Nature* **2007,** *448* (7155), 767-774.

6. Chen, Y.; Shen, Y.; Sun, D.; Zhang, H.; Tian, D.; Zhang, J.; Zhu, J. J. Fabrication of a Dispersible Graphene/Gold Nanoclusters Hybrid and Its Potential Application in Electrogenerated Chemiluminescence. *Chem. Commun.* **2011,** *47* (42), 11733-11735.

7. Nguyen, C. T.; Kasi, R. M. Nanocomposite Hydrogels Based on Liquid Crystalline Brush-Like Block Copolymer-Au Nanorods and Their Application in H_2O_2 Detection. *Chem. Commun.* **2015,** *51* (61), 12174-12177.

8. Zhao, Q.; Chen, S.; Huang, H.; Zhang, L.; Wang, L.; Liu, F.; Chen, J.; Zeng, Y.; Chu, P. K. Colorimetric and Ultra-Sensitive Fluorescence Resonance Energy Transfer Determination of H_2O_2 and Glucose by Multi-Functional Au Nanoclusters. *Analyst* **2014,** *139* (6), 1498-1503.

9. Kim, E.; Arul, N. S.; Yang, L.; Han, J. I. Electroless Plating of Copper Nanoparticles on PET Fiber for Non-Enzymatic Electrochemical Detection of H_2O_2. *RSC Adv.* **2015,** *5* (94), 76729-76732.

10. Chakraborty, S.; Raj C. R. Pt Nanoparticle-Based Highly Sensitive Platform for the Enzyme-Free Amperometric Sensing of H_2O_2, *Biosens. Bioelectron.* **2009**, *24*, 3264-3268.

11. Jena, B. K.; Raj C. R. Enzyme Integrated Silicate–Pt Nanoparticle Architecture: A Versatile Biosensing Platform, *Biosens. Bioelectron.* **2009**, *24*, 2960-2966.

12. Dey, R. S.; Raj C. R. Development of an Amperometric Cholesterol Biosensor Based on Graphene-Pt Nanoparticle Hybrid Material, *J. Phys. Chem. C* **2010**, *114*, 21427–21433.

13. Long, D. D.; Marx, K. A.; Zhou, T. Amperometric Hydrogen Peroxide Sensor Electrodes

Coated with Electropolymerized Tyrosine Derivative and Phenolic Films, *J. Electroanal. Chem.* **2001**, *501*, 107-113.

14. Senthamizhan, A.; Balusamy, B.; Aytac, Z.; Uyar, T. Ultrasensitive Electrospun Fluorescent Nanofibrous Membrane for Rapid Visual Colorimetric Detection of H_2O_2. *Anal Bioanal Chem* **2016,** *408* (5), 1347-1355.

15. Zhang, Q. M.; Guo, S.; Duan, J.; Serpe, M. J., Ordered Responsive Materials for Sensing Applications. In *Photonic Materials for Sensing, Biosensing and Display Devices*, Springer: 2016; pp 1-31.

16. Cai, Z.; Luck, L. A.; Punihaole, D.; Madura, J. D.; Asher, S. A. Photonic Crystal Protein Hydrogel Sensor Materials Enabled by Conformationally Induced Volume Phase Transition. *Chem. Sci.* **2016,** *7*, 4557-4562.

17. Cai, Z.; Kwak, D. H.; Punihaole, D.; Hong, Z.; Velankar, S. S.; Liu, X.; Asher, S. A. A Photonic Crystal Protein Hydrogel Sensor for Candida Albicans. *Angew. Chem. Int. Ed.* **2015,** *54* (44), 13036-13040.

18. Cai, Z.; Smith, N. L.; Zhang, J.-T.; Asher, S. A. Two-Dimensional Photonic Crystal Chemical and Biomolecular Sensors. *Anal. Chem.* **2015,** *87* (10), 5013-5025.

19. Griffete, N.; Frederich, H.; Maître, A.; Chehimi, M. M.; Ravaine, S.; Mangeney, C. Photonic Crystal pH Sensor Containing a Planar Defect for Fast and Enhanced Response. *J. Mater. Chem.* **2011,** *21* (34), 13052-13055.

20. Wang, F.; Zhu, Z.; Xue, M.; Xue, F.; Wang, Q.; Meng, Z.; Lu, W.; Chen, W.; Qi, F.; Yan, Z. Cellulose Photonic Crystal Film Sensor for Alcohols. *Sens. Actuators, B* **2015,** *220*, 222-226.

21. Zhong, Q.; Xie, Z.; Ding, H.; Zhu, C.; Yang, Z.; Gu, Z Carbon Inverse Opal Rods for Nonenzymatic Cholesterol Detection. *Small* **2015,** *11* (43), 5766-5770.

22. Cai, Z.; Kwak, D. H.; Punihaole, D.; Hong, Z.; Velankar, S. S.; Liu, X.; Asher, S. A. A Photonic Crystal Protein Hydrogel Sensor for Candida Albicans. *Angew. Chem. Int. Ed.* **2015,** *54* (44), 13036-13040.

23. Hou, J.; Zhang, H.; Yang, Q.; Li, M.; Jiang, L.; Song, Y. Hydrophilic-Hydrophobic Patterned Molecularly Imprinted Photonic Crystal Sensors for High-Sensitive Colorimetric Detection of Tetracycline. *Small* **2015,** *11* (23), 2738-2742.

24. Sorrell, C. D.; Serpe, M. J. Reflection Order Selectivity of Color‐Tunable Poly (N‐

isopropylacrylamide) Microgel Based Etalons. *Adv. Mater.* **2011,** *23* (35), 4088-4092.

25. Sorrell, C. D.; Carter, M. C.; Serpe, M. J. Color Tunable Poly (N‐Isopropylacrylamide)‐co‐Acrylic Acid Microgel–Au Hybrid Assemblies. *Adv. Funct. Mater.* **2011,** *21* (3), 425-433.

26. Hu, L.; Serpe, M. J. Controlling the Response of Color Tunable Poly (N-isopropylacrylamide) Microgel-Based Etalons with Hysteresis. *Chem. Commun.* **2013,** *49* (26), 2649-2651.

27. Zhang, Q. M.; Berg, D.; Mugo, S. M.; Serpe, M. J. Lipase-Modified pH-Responsive Microgel-Based Optical Device for Triglyceride Sensing. *Chem. Commun.* **2015,** *51* (47), 9726-9728.

28. Zhang, Q. M.; Xu, W.; Serpe, M. J. Optical Devices Constructed from Multiresponsive Microgels. *Angew. Chem. Int. Ed.* **2014,** *53* (19), 4827-4831.

29. Zhang, Q. M.; Wang, W.; Su, Y.-Q.; Hensen, E. J.; Serpe, M. J. Biological Imaging and Sensing with Multiresponsive Microgels. *Chem. Mater.* **2015,** *28* (1), 259-265.

30. Zhang, Q. M.; Ahiabu, A.; Gao, Y.; Serpe, M. J. CO_2-Switchable Poly (N-isopropylacrylamide) Microgel-Based Etalons. *J. Mater. Chem. C* **2015,** *3* (3), 495-498.

31. Islam, M. R.; Serpe, M. J. Label-Free Detection of Low Protein Concentration in Solution Using a Novel Colorimetric Assay. *Biosens. Bioelectron.* **2013,** *49*, 133-138.

32. Islam, M. R.; Serpe, M. J. A Novel Label-Free Colorimetric Assay for DNA Concentration in Solution. *Anal. Chim. Acta* **2014,** *843*, 83-88.

33. Zhang, Q. M.; Li, X.; Islam, M. R.; Wei, M.; Serpe, M. J. Light Switchable Optical Materials from Azobenzene Crosslinked Poly (N-isopropylacrylamide)-Based Microgels. *J. Mater. Chem. C.* **2014,** *2* (34), 6961-6965.

34. Xu, Y.; Wang, L.; Li, Y.-K.; Wang, C.-Q. Oxidation and pH Responsive Nanoparticles Based on Ferrocene-Modified Chitosan Oligosaccharide for 5-Fluorouracil Delivery. *Carbohydr. Polym.* **2014,** *114*, 27-35.

35. Hempenius, M. A.; Cirmi, C.; Song, J.; Vancso, G. J. Synthesis of Poly (ferrocenylsilane) Polyelectrolyte Hydrogels with Redox Controlled Swelling. *Macromolecules* **2009,** *42* (7), 2324-2326.

36. Gautam, D. K.; Misro, M.; Chaki, S.; Sehgal, N. H_2O_2 at Physiological Concentrations Modulates Leydig Cell Function Inducing Oxidative Stress and Apoptosis. *Apoptosis* **2006,** *11* (1), 39-46.

37. Pal, S.; Sharma, M. K.; Danielsson, B.; Willander, M.; Chatterjee, R.; Bhand, S. A Miniaturized Nanobiosensor for Choline Analysis. *Biosens. Bioelectron.* **2014,** *54*, 558-564.

38. Sardesai, N. P.; Ganesana, M.; Karimi, A.; Leiter, J. C.; Andreescu, S. Platinum-Doped Ceria Based Biosensor for in Vitro and in Vivo Monitoring of Lactate During Hypoxia. *Anal. Chem.* **2015,** *87* (5), 2996-3003.

39. Rabti, A.; Argoubi, W.; Raouafi, N. Enzymatic Sensing of Glucose in Artificial Saliva Using a Flat Electrode Consisting of a Nanocomposite Prepared From Reduced Graphene Oxide, Chitosan, Nafion and Glucose Oxidase. *Microchim. Acta* **2016,** *183* (3), 1227-1233.

40. Kasai, S.; Shiku, H.; Torisawa, Y. S.; Noda, H.; Yoshitake, J.; Shiraishi, T.; Yasukawa, T.; Watanabe, T.; Matsue, T.; Yoshimura, T. Real-time Monitoring of Reactive Oxygen Species Production During Differentiation of Human Monocytic Cell Lines (THP-1). *Anal. Chim. Acta* **2005,** *549* (1–2), 14-19.

41. Zhang, H.; Peng, L.; Xin, Y.; Yan, Q.; Yuan, J. Stimuli-Responsive Polymer Networks with Beta-Cyclodextrin and Ferrocene Reversible Linkage Based on Linker Chemistry. *Macromol. Symp.* **2013,** *329* (1), 66-69.

Table of Contents

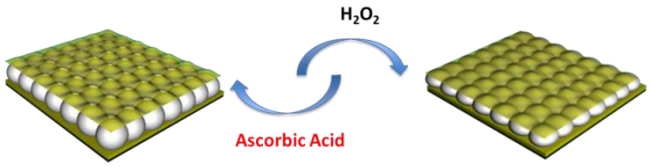

An optical device was constructed using ferrocene-modified poly (N-isopropylacrylamide) - based microgels. The devices were shown to exhibit optical properties that depended on H_2O_2 concentration. H_2O_2 generated by the reaction of glucose with glucose oxidase could also be detected and used to quantify glucose concentration in a sample. Finally, the device could be regenerated by exposure to ascorbic acid and reused.